Research Repository UCD

Title	Dinuclear ruthenium complexes containing a new ditopic phthalazin- bis(triazole) ligand that promotes metal-metal interactions
Authors(s)	Aguiló, Joan, Naeimi, Atena, Bofill, Roger, Müller-Bunz, Helge, Albrecht, Martin, et al.
Publication date	2014-05-01
Publication information	Aguiló, Joan, Atena Naeimi, Roger Bofill, Helge Müller-Bunz, Martin Albrecht, and et al. "Dinuclear Ruthenium Complexes Containing a New Ditopic Phthalazin- Bis(Triazole) Ligand That Promotes Metal-Metal Interactions." Royal Society of Chemistry, May 1, 2014. https://doi.org/10.1039/c3nj01209c.
Publisher	Royal Society of Chemistry
Item record/more information	http://hdl.handle.net/10197/6608
Publisher's version (DOI)	10.1039/c3nj01209c

Downloaded 2026-05-01 23:51:34

The UCD community has made this article openly available. Please share how this access benefits you. Your story matters! (@ucd_oa)

© Some rights reserved. For more information

Dynamic Article Links ►

Cite this: DOI: 10.1039/c0xx00000x

www.rsc.org/xxxxxx

ARTICLE TYPE

Dinuclear ruthenium complexes containing a new ditopic phthalazin-bis(triazole) ligand that promotes metal–metal interactions

Joan Aguiló,[a,b,c] Atena Naeimi,[a] Roger Bofill,[a] Helge Mueller-Bunz,[c] Antoni Llobet,[a,b] Lluís Escriche,*[a] Xavier Sala,*[a] and Martin Albrecht*[c]

Received (in XXX, XXX) Xth XXXXXXXXX 20XX, Accepted Xth XXXXXXXXX 20XX

DOI: 10.1039/b000000x

Much attention has been drawn on heterocyclic N-containing ligands due to their applicability as bridging ligands in the synthesis of redox active dinuclear metal complexes. With this aim, we report the synthesis and full characterization of a novel phthalazine-triazole ligand (1,4-bis(1-methyl-1*H*-1,2,3-triazol-4-yl)phthalazine). Moreover, we show that the phthalazine nitrogen atoms of this N-heterocyclic ligand are more reactive towards alkylating agents than the triazole groups. New ruthenium(II) complexes containing this ligand have been obtained and characterized both structurally and electrochemically. The geometry imposed by the ligand allows the placement of two ruthenium centers in very close proximity so that efficient through-space interactions take place, a concept of crucial importance for electron transfer processes.

Introduction

Ruthenium complexes with chelating heterocyclic N-donor ligands have received much attention owing to their interesting spectroscopic, photophysical and electrochemical properties.[1] The redox-active nature of those complexes makes them conceivable mediators of electron transfer in photochemical processes, leading to potential uses in diverse areas such as photosensitizers for photochemical conversion of solar energy,[2] molecular electronic devices[3] and photoactive DNA cleavage agents for therapeutic purposes.[4] Furthermore, this broad family of complexes has been shown to act as excellent catalysts in CO_2 reduction, enantioselective hydrogenation, alcohol oxidation, epoxidation, sulfoxidation and water oxidation processes.[5–7]

Specific attention has been directed to ditopic *N*-heterocyclic ligands due to their applicability as bridging ligands in the synthesis of dinuclear metal complexes.[3] The metal properties in such systems are directly related to the nature of the bridging ligand, which offers a methodology for tailoring of, for example, the electronic communicaton between the metal centers. Additionally, the nature and topology of the ligand can trigger mutual cooperativity of the two coordinated metals through space.[8] The degree of electronic coupling between the metal centers and also synergistic intermetallic properties directly depend on the extent of interaction of the bridging ligand orbitals with those of the metal centers.[9] Furthermore, the presence of non-bridging spectator ligands can be used to influence the relative energies of the metal-based orbitals, and these ligands are therefore able to indirectly fine-tune the electronic communication between the two metal centers.[10] For example, the heterocyclic bridging ligand 3,5-bis(2-pyridyl)pyrazole (H-bpp, Fig. 1) with four *N*-donor sites was used to prepare the dinuclear ruthenium(II) complex $\mathbf{C}^{2+}$ (Fig. 1c).[6] Once bridged by the anionic bpp$^-$ ligand, the rigidly meridional coordination geometry of the terpy ligands induce through-space interactions between the two ruthenium sites.[11] However, the arrangement of the coordinating heterocyclic rings in H-bpp, specifically the presence of a central five-membered pyrazole with the two six-membered pyridine rings on each side, induced considerable strain when accommodating two ruthenium(II) centers, as evidenced by an appreciable distortion of the Ru–N–N–Ru dihedral angle (Fig. 1b).

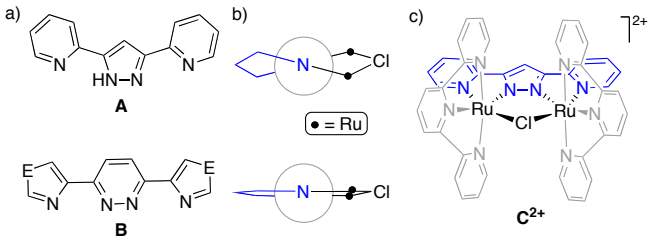

Fig. 1 a) Two options **A** (H-bpp) and **B** for arranging 5- and 6-membered heterocycles around a central ditopic *N,N*-unit; b) Newman projection along the N–N axis of the central ditopic *N,N*-unit emphasizing the steric strain induced by the five-membered central ring with 6-membered heterocycles at the periphery, while the inverse arrangement (bottom) induces an almost ideal co-axial arrangement of the Ru…Ru vector with the N–N bond of the central unit; c) representative complex $\mathbf{C}^{2+}$ with the monoanionic bpp$^-$ ligand and substantial torsion (Ru–N–N–Ru ca. 19°).

Based on these considerations, we have now designed and prepared a ditopic N_2,N_2-coordinating ligand that features a six-membered central ring and two five-membered heterocycles in adjacent positions. This geometry is expected to be better suited for accommodating two Ru(II) ions in the ligand plane (Fig. 1a,b

This journal is © The Royal Society of Chemistry [year]

bottom). As a consequence, the coordination axes of the two ruthenium centers are better mutually aligned, which will facilitate metal-metal interactions due to enhanced orbital overlap. Here, we report the synthesis and characterization of a novel phthalazine-triazole ligand (1,4-bis(1-methyl-1*H*-1,2,3-triazol-4-yl)phthalazine) and its coordination properties to octahedral ruthenium(II) centers. Due to the optimized coordination geometry and the ensuing electronic coupling of the metal centers, the bimetallic complexes demonstrate a broad potential window for stabilizing the mixed-valent species.

Results and discussion

Ligand synthesis and characterization

The synthesis of the target ligand started from 1,4-diiodophthalazine[12] as the central six-membered heterocycle. Sonogashira cross-coupling with trimethylsilylacetylene according to a previously reported methodology[13] and using Cs_2CO_3 as a mild base[14] afforded 1,4-bis(trimethylsilyl-ethynyl)phthalazine (**1**) in moderate yield. A double [3+2] cycloaddition ("click" reaction)[15] between **1** and methyl azide, generated in situ from sodium azide and methyl iodide, subsequently afforded the target ligand 1,4-bis(1-methyl-1*H*-1,2,3-triazol-4-yl)phthalazine (**2**). While click reactions typically involve terminal alkynes as reactants,[16] we employed here a one-step procedure that involves K_2CO_3-induced deprotection of the alkyne[17] and copper-catalyzed cycloaddition in the presence of ascorbate in one pot. Reactions under microwave conditions increase both the reaction rate and the product yield as compared to conventional heating.[18] According to this procedure and after extensive washing to remove residual copper salts,[19] pure ligand **2** was obtained in good 80% yield from precursor **1** (Scheme 1).

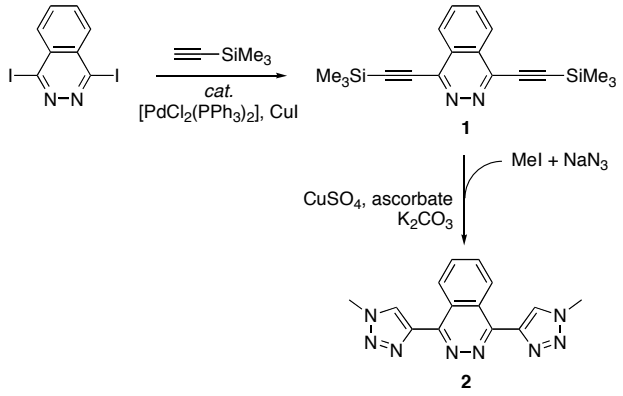

Scheme 1 Synthesis of ligand precursor **2**.

The purity of compounds **1** and **2** was confirmed by NMR spectroscopy, ESI-MS (Fig. S1–S3) and elemental analysis (see the Experimental Section). One- and two-dimensional NMR experiments proved valuable for full structural characterization of the compounds in solution. Both compounds **1** and **2** display C_{2v} symmetry in solution, which mutually relates the two alkyne substituents of **1** and the two triazole rings of **2** by symmetry. The aryl protons H7 and H8 of the phthalazine unit appear as doublet of doublets (inset Fig. S1a), which is in agreement with the typical AA'BB' pattern for such systems. The pertinent coupling constants are larger for $J_{7,8}$ = 6.3 Hz than for $J_{7,8'}$ = 3.3 Hz. The assignment of H7 and H8 was unambiguously confirmed by long-range coupling to C6 and C4 (Figure S1e).

The most characteristic NMR feature of ligand **2** pertains to the triazole protons, which appear as one singlet at δ_H 8.70 ppm, demonstrating the successful cycloaddition on both sides of the phthalazine unit. Moreover, ligand **2** displays a downfield shift of the doublet of doublets attributed to H7 as a consequence of the aromaticity of the triazole ring (Fig. S3).

Reactivity in methylation reactions

The relative donor ability of the nitrogen sites in compound **2** have been assessed by probing their nucleophilicity towards CH_3^+ electrophiles. Even though phthalazines are less basic than triazoles (pK_b = 10.5 and 9.4, respectively),[20] alkylation of **2** occurred predominantly at the phthalazine site and produced selectively the mono- and dicationic salts $\mathbf{3}^+$ and $\mathbf{4}^{2+}$, respectively (Scheme 2). Thus, when **2** was reacted with MeI as alkylating agent in MeCN at 80 ºC, the monocationic iminium salt $\mathbf{3}^+$ was produced exclusively due to methylation of one of the phthalazine nitrogen atoms. Results after 3 h were identical to those at longer reaction times and after addition of further portions of MeI. However, when **2** was reacted with MeOTf (OTf = trifluoromethyl sulfonate) as stronger alkylating agent in CH_2Cl_2 at 45 °C a double methylation was observed, which involved the phthalazine and one of the triazole units, yielding $\mathbf{4}^{2+}$. The preference for phthalazine alkylation and formation of $\mathbf{3}^+$ indicates a higher nucleophilicity of these central nitrogen atoms as compared to the triazole nitrogens. The selectivity of the second methylation towards the triazole unit is a direct consequence of the reduced electron density in the phthalazine ring after the first alkylation. Selective alkylation of the triazole distal to the methylated phthalazine nitrogen is probably induced by steric congestion similar to ortho-substituted biaryls, and inductively due to the presence of the iminium cation.

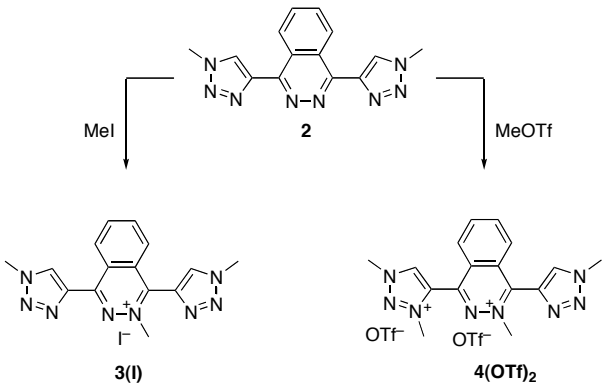

Scheme 2 Synthesis of the iminium salts $\mathbf{3}^+$ and $\mathbf{4}^{2+}$.

Both alkylated products $\mathbf{3}^+$ and $\mathbf{4}^{2+}$ were characterized by NMR spectroscopy (Fig. S4, S5). The asymmetric alkylation of the N atoms in $\mathbf{3}^+$ and $\mathbf{4}^{2+}$ induces a loss of symmetry, which results in a more complicated set of NMR resonances than **2**. Thus, H7 and H8 (see Fig 2 for atom labelling scheme) do not appear as a AA'BB' spin system and become regular doublets and triplets, respectively. In $\mathbf{4}^{2+}$, the triazolium proton H14 is deshielded by 0.5 ppm compared the equivalent proton (H2) of the neutral triazole ring. Only a single set of resonances was observed, which points to regioselective alkylation of the

nitrogen α to the substituted triazole carbon.[21] The structures of these alkylated products was unambiguously confirmed by X-ray diffraction analysis of suitable single crystals, which were obtained by slow evaporation of $CDCl_3$ and CD_3CN solutions of $\mathbf{3}^{+}$ and $\mathbf{4}^{2+}$, respectively. Fig. 2 displays the molecular structures and the corresponding atom labelling scheme (see Fig. S11–S14 and Tables S1,S2 for further views and crystallographic details).

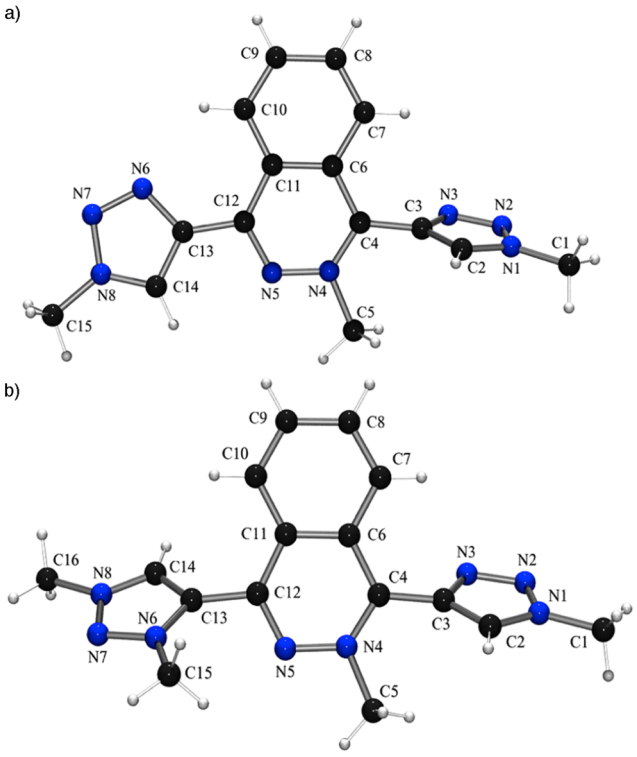

Fig. 2 POV-RAY plot of $\mathbf{3}^{+}$ (a) and $\mathbf{4}^{2+}$ (b) and adopted atom labelling schemes (OTf^- anions and co-crystallized solvent molecules omitted for clarity).

The molecular structure of $\mathbf{3}^{+}$ is characterized by two planes, one comprised of the coplanar phthalazine moiety and the distal triazole ring (torsion angle N5–C12–C13–C14 = 8.9(5)°), and the other plane defined by the proximal triazole heterocycle adjacent to the phthalazinium N–CH_3 group. The planes are significantly tilted as demonstrated by the large torsion angle N4–C4–C3–C2 = 75.5(5)°. This almost perpendicular orientation is presumably imparted by repulsion between the triazole proton (H2) and the N-bound methyl group (H5). Accordingly, all three heterocycles of the dicationic compound $\mathbf{4}^{2+}$ are mutually twisted in the solid state structure (Fig. 2b). The torsion angles between both triazole rings and the central phthalazine scaffold are N4–C4–C3–C2 = 51.1(12)° and N5–C12–C13–C14 = 42.9(8)°. Interestingly, no N–CH_3…N close contacts were observed in either compound that might point to intramolecular hydrogen bonding. Finally, we note that the torsion angles between the phthalazinium unit and triazole rings are variable (from 43° to 75°). This steric flexibility is particularly useful for metal coordination.

Ruthenium(II) complexation

Ligand **2** was used as a N_2,N_2-bridging ligand in order to obtain a dinuclear Ru^{II},Ru^{II} complex. Thus, complexation of **2** with $[RuCl_3(terpy)]$ (terpy = 2,2':6',2"-terpyridine) as starting material in MeOH at reflux temperature in the presence of slightly over-stoichiometric quantities of Et_3N and LiCl induced reduction of the metal center to the +2 oxidation state and simultaneously coordination of **2**, thus affording complexes $[Ru_2(\mu\text{-}Cl)(\mathbf{2})(terpy)_2]^{3+}$ ($\mathbf{5}^{3+}$) and $[Ru^{II}(Cl)(\mathbf{2})(terpy)]^{+}$ ($\mathbf{6}^{+}$; Scheme 3 and Fig. S6). These two products were successfully separated by column chromatography using alumina with a mixture of CH_2Cl_2 and MeOH (99:1) as eluent, providing the dinuclear complex $\mathbf{5}^{3+}$ as the major product (20% yield based on ruthenium) and the monometallic complex $\mathbf{6}^{+}$ as a minor fraction (<5% yield).

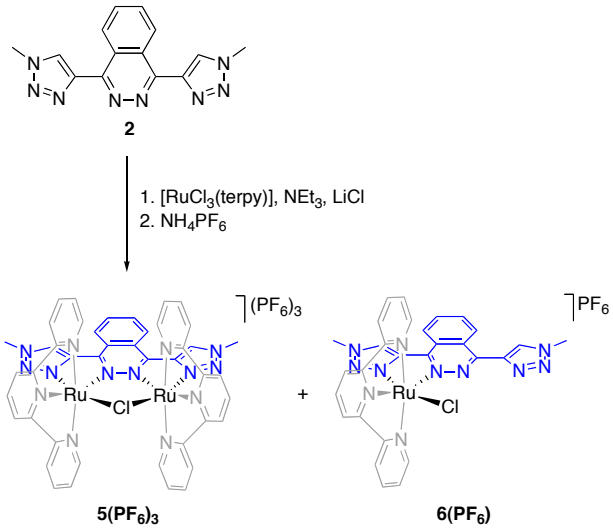

Scheme 3 Synthesis of bimetallic complex $\mathbf{5}^{3+}$ and mononuclear $\mathbf{6}^{+}$.

In solution, complex $\mathbf{5}^{3+}$ displays C_{2v} symmetry as indicated by the simple resonance pattern observed for the complex (Fig. S7). The terminal pyridyl rings of the two terpy ligands are all symmetry-related and appear as one single set of four resonances. Coordination of the triazole rings to the ruthenium(II) centers was deduced from the 1.2 ppm downfield shift of the H2 singlet in the ^{1}H NMR spectrum (δ_H 9.94 ppm) as compared to the frequency in the free ligand **2** (δ_H 8.70 ppm). This chemical shift difference reflects to some extent the depletion of electron density in the triazole ring due to *N*-coordination to the ruthenium(II) center. Of note, the deshielding is much stronger than in the dicationic compound $\mathbf{4}^{2+}$, presumably because the heterocycles are mutually planar in $\mathbf{5}^{3+}$ due to chelation (see structural discussion below), which entails mesomeric effects that are suppressed in the out-of-plane tilting of the heterocycles in $\mathbf{4}^{2+}$. The purity of $\mathbf{5}^{3+}$ was confirmed by ESI-MS and elemental analysis.

In contrast to $\mathbf{5}^{3+}$, the ^{1}H NMR spectrum of $\mathbf{6}^{+}$ (Figure S8) shows no symmetry. The four protons of the central phthalazine scaffold appear as doublets and triplets. In addition, the triazole N–CH_3 substituents are no longer equivalent and appear as two distinct singlet resonances at δ_H 4.2 and 4.7 ppm. Similarly, two singlets are observed for the triazole CH protons at δ_H 7.5 and 10.1 ppm. The integral ratio between the signals of the terpy ligand and the phthalazine as well as the shift of only one triazole proton resonance to higher frequency is in good agreement with the coordination of a monometallic complex where only one half of the phthalazine-triazole scaffold is coordinated to a Ru(terpy) unit. Coordination to the phthalazine nitrogen is in good agreement with this nitrogen being the most nucleophilic center

as observed with the formation of the monoalkylated compound $\mathbf{3}^{+}$. This similarity thus validates the alkylation experiments as useful probes for metal coordination to ligand **2**.

Electrochemical and structural analysis of the complexes

The redox properties of complexes $\mathbf{5}^{3+}$ and $\mathbf{6}^{+}$ were investigated by means of cyclic voltammetry (CV) in acetone (Fig. S10). The cyclic voltammogram of $\mathbf{5}^{3+}$ exhibits two reversible waves that were assigned to the consecutive oxidation of the two ruthenium centers according to Eq. 1 and 2 (**2** and terpy ligands not shown for clarity):

$$[Ru^{III}(\mu\text{-}Cl)Ru^{II}]^{4+} + 1e^{-} \rightarrow [Ru^{II}(\mu\text{-}Cl)Ru^{II}]^{3+} \quad (+0.83\ V) \quad (1)$$

$$[Ru^{III}(\mu\text{-}Cl)Ru^{III}]^{5+} + 1e^{-} \rightarrow [Ru^{III}(\mu\text{-}Cl)Ru^{II}]^{4+} \quad (+1.27\ V) \quad (2)$$

These two $E_{1/2}$ values (*vs.* SSCE) confirm the existence of electronic communication between both Ru centers, and are similar to the 0.79 V and 1.20 V half-wave redox potentials reported for the related bpp-bridged bimetallic complex $\mathbf{C}^{2+}$ (*cf* Fig. 1).[6] This very similar electrochemical behavior of these two complexes is presumably a consequence of the specific donor properties of the two bridging ligands. Hence, the lower σ-donating character of the neutral phthalazine unit in $\mathbf{5}^{3+}$ as compared to the monoanionic pyrazolate ring in the bpp-bridged complex is counterbalanced by the higher σ-donor properties of the triazole donors in $\mathbf{5}^{3+}$ *vs* the pyridine rings in the bpp ligand. The two oxidation processes are slightly more separated in $\mathbf{5}^{3+}$ than in $\mathbf{C}^{2+}$ (ΔE = 0.44 mV *vs* 0.41 mV), which translates into a modestly higher comproportionation constant K_C.

The mononuclear complex $\mathbf{6}^{+}$ shows a single reversible wave, which was assigned to the following $Ru^{III/}Ru^{II}$ redox process:

$$[Ru^{III}(Cl)(\mathbf{2})(terpy)]^{2+} + 1e^{-} \rightarrow [Ru^{II}(Cl)(\mathbf{2})(terpy)]^{+} \quad (+0.86\ V) \quad (3)$$

This $E_{1/2}$ value is essentially identical to that of structurally related $[Ru^{II}(N_5Cl)]^{+}$ mononuclear complexes, such as $[Ru^{II}(terpy)(bpy)(Cl)]^{+}$ (+0.80 V *vs.* SSCE)[22] or *in*-$[Ru^{II}(Hbpp)(terpy)(Cl)]^{+}$ (+0.86 V *vs.* SSCE),[7] thus further supporting the proposed structure for $\mathbf{6}^{+}$. Moreover, given the fact that the *out* isomer of $[Ru^{II}(Hbpp)(terpy)(Cl)]^{+}$ shows a significantly lower $E_{1/2}$ potential (+0.63 V *vs.* SSCE),[7] complex $\mathbf{6}^{+}$ most probably also features an *in* conformation (*i.e.* the chloride ligand is *trans* to the triazole ligand and not *trans* to the phthalazine nitrogen).

Suitable crystals for X-ray diffraction analysis were obtained for $\mathbf{5(PF_6)_3}$. Figure 3 displays a POV-RAY plot of the cationic complex with the corresponding labelling scheme (see also Table S3 and Fig. S15). Complex $\mathbf{5(PF_6)_3}$ crystallizes in a small cell containing two complex molecules, two molecules of acetone and six PF_6^{-} anions. Each ruthenium center features a pseudo-octahedral coordination geometry with two positions occupied by ligand **2**, three positions by the meridional terpy ligand and the sixth site filled with a bridging chloride ligand. The complex cation has crystallographic C_{2v} symmetry as deduced from solution analysis, with one symmetry plane containing ligand **2**, the two ruthenium atoms, both central terpyridine nitrogen atoms and the bridging chloride. A second plane perpendicularly bisects the other plane and passes through the chloride center and through the middle of the N4–N4', C5–C5' and C7–C7' bonds of the phthalazine scaffold, thus mutually relating the two terpy ligands by symmetry.

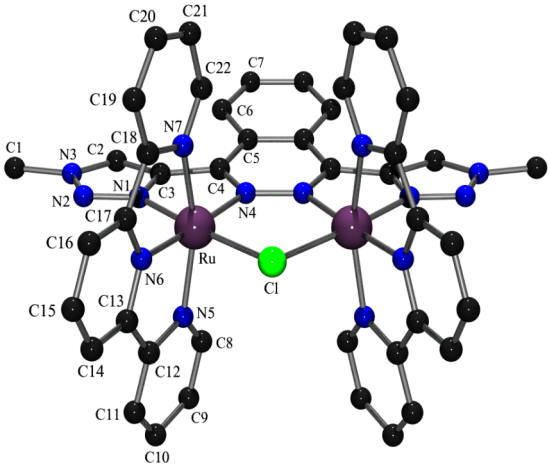

Fig. 3 POV-RAY plot of $\mathbf{5}^{3+}$ with adopted atom labelling scheme (PF_6^{-} anions and co-crystallized solvent molecules omitted for clarity).

It is instructive to compare the structure of $\mathbf{5}^{3+}$ with those of related bimetallic ruthenium complexes such as complex $\mathbf{C}^{2+}$ (*cf* Fig. 1c)[6] and with complex $\mathbf{D}^{+}$,[23] which comprises six-membered heterocycles at the periphery of the phthalazine core (Fig. 4). Moreover, the terpy ligand in the latter complex is replaced by a chelating carboxylate ligand and two axial unsupported picoline groups.

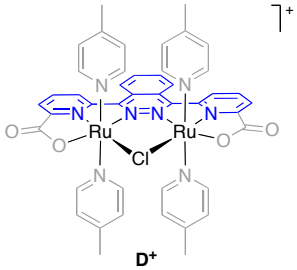

Fig. 4 Schematic representation of $\mathbf{D}^{+}$.

The most relevant structural features around the metal centers (bond distances and angles) of all three complexes are listed in Table 1. Replacement of the five-membered pyrazole unit in $\mathbf{C}^{2+}$ with a six-membered phthalazine ring in $\mathbf{5}^{3+}$ results in longer Ru–N4 bonds and shorter Ru–Ru' and Ru–Cl distances. These changes are also reflected in the 5° smaller Ru–Cl–Ru' angle in $\mathbf{5}^{3+}$. All these differences are in agreement with the expected better accommodation of the two ruthenium(II) centers in $\mathbf{5}^{3+}$ due to the presence of a six-membered central heterocycle when compared with the bpp^{-} ligand scaffold. Specifically, this less constrained situation induces an undistorted Ru–N4–N4'–Ru' dihedral angle (0°), while in $\mathbf{C}^{2+}$ the ruthenium coordination axis are severly distorted as demonstrated by the large dihedral angle (Ru–N4–N4'–Ru' = 18.69°).

Table 1 Selected bond lengths (Å) and angles (°) for $\mathbf{5}^{3+}$ and the related complexes $\mathbf{C}^{2+}$ and $\mathbf{D}^{+}$

	$\mathbf{5}^{3+}$	$\mathbf{C}^{2+}$ [a,c]	$\mathbf{D}^{+}$ [b,c]
Ru–N1	1.993(4)	2.054(3)	1.925(10)
Ru–N4	2.089(4)	1.999(3)	1.995(10)
Ru–N5	2.069(4)	2.079(4)	2.080(11)
Ru–N6	1.966(4)	1.967(3)	n.a.
Ru–N7	2.068(5)	2.060(3)	2.085(10)
Ru–Cl	2.396(12)	2.4466(7)	2.438(3)
Ru'–Cl	2.396(12)	2.4466(7)	2.432(3)
Ru–Ru'	3.657	3.876	3.576
Ru–Cl–Ru'	99.84(6)	104.77(4)	94.51(11)
N5–Ru–N7	158.77(15)	158.15(14)	171.8(4)
Ru–N4–N4'–Ru'	0.0	18.7	4.7

[a] from ref. 6; [b] from ref. 23; [c] atom numbering adapted to $\mathbf{5}^{3+}$ (Fig. 3).

Complex $\mathbf{D}^{+}$ has a bridging scaffold that may be considered as a hybrid between that of $\mathbf{5}^{3+}$ and that of $\mathbf{C}^{2+}$. The distortion of the Ru–N4–N4'–Ru' angle is small (4.70º), indicating a slightly higher strain than in $\mathbf{5}^{3+}$, which may also account for the shorter Ru–N1 and Ru–Ru' distances compared to $\mathbf{5}^{3+}$. The presence of two independent axial picoline groups per ruthenium(II) center in $\mathbf{D}^{+}$ compared to the tridentate meridional terpy ligand present in $\mathbf{5}^{3+}$ increases the N5–Ru–N7 angle from 158.77º to 171.8º, an arrangement that is closer to an ideal *trans* disposition.

Conclusions

In this work we have described the synthesis of a novel phthalazine-triazole ligand (**2**) by a Sonogashira cross-coupling reaction of iodophtalazine with an acetylene derivative, followed by a click reaction with methyl azide. Furthermore, two different methylation products of **2** were obtained ($\mathbf{3}^{+}$ and $\mathbf{4}^{2+}$), which demonstrate the nucleophilicity of the central phthalazine unit. Metalation provides a dinuclear complex $[Ru^{II}_2(\mu\text{-}Cl)(\mathbf{2})(terpy)_2]^{3+}$ ($\mathbf{5}^{3+}$) featuring **2** as a bis(chelating) N_2,N_2-coordinating ligand, as well as the mononuclear compound $[Ru^{II}(Cl)(\mathbf{2})]^{+}$ ($\mathbf{6}^{+}$). Electrochemical data on $\mathbf{5}^{3+}$ indicate strong electronic communication between the two ruthenium centers, and X-Ray diffraction studies demonstrate an excellent accommodation of both metal centers, since the phthalazine-triazole scaffold displays a completely planar conformation. Further work will be directed towards exploiting the catalytic potential of $\mathbf{5}^{+}$ and $\mathbf{6}^{3+}$ in various redox processes in order to evaluate whether structural optimization also induces improved activity. Moreover, the optimized ligand structure should also benefit the mutual arrangement of other (hetero-)bimetalic structures, thus providing access to a novel scaffold for cooperative catalysis and self-assemblies such as coordination polymers.

In addition, the triazolium salts obtained from alkylation of the peripheral heterocycle afford potentially chelating abnormal carbene precursors, which have been established as powerful ligands for metal-catalyzed oxidation reactions.[24] The incorporation of such triazolylidene ligands into multimetallic systems may constitute a promising approach for improving catalytic activity.

Experimental section

General

Materials. All reagents used in the present work were obtained from Aldrich Chemical Co. and were used without further purification. Reagent-grade organic solvents were obtained from Scharlab. $RuCl_3{\cdot}3H_2O$ was supplied by Alfa Aesar and was used as received. The starting ligand 1,4-diiodophthalazine,[12] $[PdCl_2(PPh_3)_2]$,[25] and $[RuCl_3(terpy)]$[26] were prepared as described in the literature. All synthetic manipulations were routinely performed under nitrogen atmosphere using Schlenk tubes and vacuum-line techniques.

Equipment and analyses. NMR spectroscopy was performed on a Bruker DPX 250 MHz, DPX 360 MHz or a DPX 400 MHz spectrometer or in a Varian 500 MHz or 300 MHz NMR System. Samples were run in $CDCl_3$, CD_3CN or acetone-D_6 with internal references. Electrospray ionization mass spectrometry (ESI-MS) measurements were carried out on an HP298s gas chromatography (GC-MS) system from the SAQ-UAB. Cyclic voltammetry experiments were performed on an Ij-Cambria HI-660 potentiostat using a three-electrode cell. A glassy carbon electrode (2 mm diameter) was used as working electrode, platinum wire as auxiliary electrode and a SSCE as a reference electrode. Working electrodes were polished with 0.05 micron Alumina paste washed with distilled water and acetone before each measurement. The complex was dissolved in acetone containing the necessary amount of n-Bu_4NPF_6 as supporting electrolyte to yield 0.1 M ionic strength solution. $E_{1/2}$ values reported in this work were estimated from CV experiments as the average of the oxidative and reductive peak potentials ($E_{p,a}$ + $E_{p,c}$)/2.

X-ray diffraction studies. Crystal data for $\mathbf{3}^{+}$, $\mathbf{4}^{2+}$ and $\mathbf{5}^{3+}$ were collected using an Oxford Diffraction SuperNova A diffractometer fitted with an Atlas detector. All samples were measured with Mo–Kα (0.71073 Å). An at least complete dataset was collected, assuming that the Friedel pairs are not equivalent. An analytical absorption correction based on the shape of the crystal was performed for all these crystals.[27] The structures were solved by direct methods using SHELXS-97[28] and refined by full matrix least-squares on F^2 for all data using SHELXL-97. Their isotropic thermal displacement parameters were fixed to 1.2 times (1.5 times for methyl groups) the equivalent one of the parent atom. Anisotropic thermal displacement parameters were used for all non-hydrogen atoms. CCDC numbers 948959-948961 contain the supplementary crystallographic data for this paper. These data can be obtained free of charge from the Cambridge Crystallographic Data Centre via www.ccdc.cam.ac.uk/data_request/cif.

Synthetic procedures

1,4-bis((trimethylsilyl)ethynyl)phthalazine (1). A mixture of Cs_2CO_3 (0.41 g, 1.3 mmol) and 1,4-diiodophthalazine (120 mg, 0.314 mmol) were cooled in a Schlenk flask to –15 °C and placed under argon by applying several vacuum/argon cycles. Dry, degassed THF (4 mL) was added *via* canula, and the mixture was flushed with argon. $PdCl_2(PPh_3)_2$ (22.1 mg, 0.031 mmol) and CuI (6 mg, 0.03 mmol) were added. The flask was degassed again, and trimethylsilylacetylene (101 μl, 0.69 mmol) was added. The

mixture was stirred for 30 min at –15 °C and 4 h at room temperature. The reaction mixture was then poured into H_2O:NH_3 (30 mL, 2:1) and the product was extracted with EtOAc (20 mL). The organic fraction was washed with H_2O:NH_3 until no more blue colour was observed. Finally, it was washed with water (2 × 20 mL) and brine (2 × 100 mL) and dried over anhydrous Na_2SO_4. After evaporation of the solvents, the solid residue was purified by column chromatography (SiO_2; hexane/EtOAc 98:2). Yield: 22 mg (20%). ^{1}H NMR (500 MHz, $CDCl_3$): δ = 8.31 (dd, 2H J_{7-8} = 6.3 Hz, $J_{7-8'}$ = 3.3 Hz, H7), 7.97 (dd, 2H, J_{8-7} = 6.3 Hz, $J_{8-7'}$ = 3.3 Hz, H8), 0.38 (s, 18H, H1). ^{13}C{^{1}H} NMR (125 MHz, $CDCl_3$): δ = 145.30 (C4), 133.55 (C7), 126.98 (C6), 126.26 (C8), 106.12 (C2), 98.97 (C3), 0.00 (C1). ESI-MS (MeOH): *m/z* = 323.14 ($[M]^+$).

1,4-bis(1-methyl-1*H*-1,2,3-triazol-4-yl)phthalazine (2). MeN_3 was generated *in situ* by stirring a mixture of MeI (76.7 μl, 1.2 mmol), sodium azide (240 mg, 3.69 mmol) and 7 mL of THF:H_2O (1:1) in a microwave flask overnight at room temperature. After that time, **1** (75 mg, 0.233 mmol), $CuSO_4{\cdot}5H_2O$ (23.22 mg, 0.093 mmol), sodium ascorbate (36.85 mg, 0.186 mmol) and K_2CO_3 (63.25 mg, 0.465 mmol) were added and the mixture was irradiated with a microwave reactor (100 W, 5 + 30 min, 100 °C). The reaction mixture was then poured into CH_2Cl_2 (50 mL) and the organic fraction was washed with H_2O:NH_3 2:1 (3 × 50 mL, until no blue copper colour was observed), H_2O (2 × 50 mL) and brine (2 × 50 mL). The organic layer was dried over anhydrous Na_2SO_4 and activated charcoal. Evaporation of all volatiles gave **2** as a yellow powder (50 mg, 80 %). ^{1}H NMR (500 MHz, $CDCl_3$): δ = 9.73 (dd, 2H, J_{7-8} = 6.3 Hz, $J_{7-8'}$ = 3.3 Hz, H7), 8.70 (s, 2H, H2), 7.97 (dd, 2H, J_{8-7} = 6.3 Hz, $J_{8-7'}$ = 3.3 Hz, H8), 4.28 (s, 6H, H1). ^{13}C{^{1}H} NMR (500 MHz, $CDCl_3$): δ = 135.21 (C8), 129.11 (C7), 128.59 (C2), 126.23 (C6), 37.36 (C1). Elemental analysis calcd for $C_{14}H_{12}N_8$: C, 57.53; H, 4.14; N, 38.34. Found: C, 57.65; H, 4.19; N, 38.16.

2-methyl-1,4-bis(1-methyl-1*H*-1,2,3-triazol-4-yl)phthalazin-2-ium iodide (3(I). Compound **2** (10 mg, 0.034 mmol) and methyl iodide (13 μl, 0.200 mmol) were heated (80 °C) in acetonitrile (7 mL) in a sealed tube for 24 h. Evaporation of the solvents and subsequent recrystallization from $CHCl_3$ yielded yellow crystals. ^{1}H NMR (500 MHz, CD_3CN): δ = 10.0 (d, 1H, J_{7-8} = 8.57 Hz, H7), 9.74 (s, 1H, H2), 8.64 (s, 1H, H14), 8.40 (t, 1H, J_{7-8} = 8.57 Hz, J_{8-9} = 7.52 Hz, H8), 8.32 (d, 1H, J_{9-10} = 8.30 Hz, H10), 8.23 (t, 1H, J_{9-10} = 8.30 Hz, J_{8-9} = 7.52 Hz, H9), 4.72 (s, 3H, H5), 4.40 (s, 3H, H15), 4.31 (s, 3H, H1). Elemental analysis calcd for $C_{16}H_{17}IN_8$ × $CHCl_3$: C, 35.97; H, 3.20; N, 18.74. Found: C, 36.01; H, 3.22; N, 18.68.

4-(1,3-dimethyl-1*H*-1,2,3-triazol-3-ium-4-yl)-2-methyl-1-(1-methyl-1*H*-1,2,3-triazol-4-yl)phthalazin-2-ium triflate (4(OTf)$_2$). Compound **2** (10 mg, 0.034 mmol) and MeOTf (40 μl, 0.34 mmol) were heated (45 °C) in CH_2Cl_2 (2 mL) in a sealed tube for 16 h. The solution was then filtered and the solid residue was washed with fresh CH_2Cl_2 and Et_2O. Recrystallization from warm MeCN yielded brown crystals of **4(OTf)$_2$**. ^{1}H NMR (500 MHz, CD_3CN): δ = 9.11 (s, 1H, H14), 8.73 (s, 1H, $H2_2$), 8.64 (m, 2H, H7-8), 8.50 (m, 2H, H9-10), 4.69 (s, 3H, H5), 4.51 (s, 3H, H16), 4.49 (s, 3H, H15), 4.37 (s, 3H, H1). ^{13}C{^{1}H} NMR (125 MHz, CD_3CN): δ = 153.82 (C4), 147.96 (C12), 140.30 (C8), 137.99 (C9), 134.22 (C14), 133.74 (C13), 133.50 (C3), 131.85 (C2), 131.55 (C7), 130.42 (C11), 127.77 (C6), 126.83 (C10), 52.00 (C5), 41.03 (C16), 40.33 (C15), 37.44 (C1). Elemental analysis calcd for $C_{18}H_{18}F_6N_8O_6S_2$: C, 34.84; H, 2.92; N, 18.06. Found: C, 34.80; H, 2.92; N, 18.10.

[Ru$^{II}_2$(μ-Cl)(2)(terpy)$_2$](PF$_6$)$_3$ (5(PF$_6$)$_3$ and **[Ru^{II}(Cl)(2)](PF$_6$)$_3$ (6(PF$_6$)).** Solid $[RuCl_3(terpy)]$ (90 mg, 0.20 mmol) and LiCl (16 mg, 0.31 mmol) were dissolved in a solution of NEt_3 (57 μl, 0.41 mmol) and dry MeOH (30 mL). The mixture was stirred at room temperature for 20 min, and then **2** (30 mg, 0.10 mmol) was added. The resulting solution was heated to 65 °C for 16 h. The reaction mixture was filtered, and then a saturated aqueous NH_4PF_6 solution (1 mL) was added to obtain a brown precipitate. The solid was collected, washed with cold water (3 × 5 mL) and Et_2O (3 × 5 mL) and finally dried under vacuum to afford a mixture of complexes. Purification by alumina chromatography (DCM:MeOH 99:1) yielded **5(PF$_6$)$_3$** (30 mg, 20%) and **6(PF$_6$)** (3 mg, 5%). Microanalytically pure crystals of **5(PF$_6$)$_3$** were obtained upon slow diffusion of Et_2O into an acetone solution of the complex. ^{1}H NMR (400 MHz, acetone–D_6): δ = 9.94 (s, 2H, H2), 9.15 (dd, 2H, J_{6-7} = 6.3 Hz, $J_{6-7'}$ = 3.3 Hz, H6), 8.67 (m, 8H, H14-8), 8.53 (d, 4H, J_{11-10} = 7.8 Hz H11), 8.47 (dd, 2H, J_{7-6} = 6.3 Hz, $J_{7-6'}$ = 3.3 Hz, H7), 8.31 (t, 2H, J_{15-14} = 9 Hz, H15), 8.00 (dd, 4H, J_{9-10} = 8.5 Hz, J_{11-10} = 7.8 Hz, H10), 7.45 (dd, 4H, J_{9-10} = 7.8 Hz, J_{9-8} = 6.3 Hz, H9), 4.14 (s, 6H, H1). ^{13}C{^{1}H} NMR (125 MHz, [D_6]acetone): δ = 158.98 (C4), 158.65 (C13), 155.46 (C8), 153.52 (C5), 148.03 (C3), 139.43 (C10), 138.04 (C15), 136.44 (C7), 132.84 (C2), 128.51 (C9), 126.21 (C12), 125.96 (C6), 125.08 (C11), 123.76 (C14), 39.5 (C1). ESI-MS (MeOH): *m/z* = 1287.0 ($[M\text{-}PF_6]^+$). Elemental analysis calcd for $C_{47}H_{44}ClF_{18}N_{14}P_3Ru_2$ × 2 C_3H_6O: C, 39.95; H, 3.54; N, 12.31. Found: C, 40.06; H, 3.52; N, 12.22. Spectroscopic data for **6(PF$_6$)**: ^{1}H NMR (400 MHz, [D_6]acetone): δ = 10.04, 9.45, 8.74, 8.69, 8.53, 8.35, 8.16, 8.03, 7.95, 7.80, 7.58, 7.53, 7.35, 4.76, 4.18. Due to the low quantitiy of product, ^{13}C NMR resonances were not sufficiently resolved.

Acknowledgements

We thank Dr. Jordi García-Antón for assistance in generating the X-Ray structure figures and Science Foundation Ireland and MINECO (CTQ2011-26440, CTQ 2010-21497 and CTQ2010-21532-C02-02) for financial support. J.A. gratefully acknowledges a PIF doctoral grant from UAB.

Notes and references

[a] *Departament de Química, Universitat Autònoma de Barcelona, Cerdanyola del Vallès, 08193, Barcelona, Catalonia, Spain. Fax: +34 5812477; E-mail: lluis.escriche@uab.cat, xavier.sala@uab.cat*

[b] *Institute of Chemical Research of Catalonia (ICIQ), Av. Països Catalans 16, 43007 Tarragona, Catalonia, Spain.*

[c] *School of Chemistry & Chemical Biology, University College Dublin, Belfield, Dublin 4, Ireland. Fax: +353 17162501; Tel: +353 17162504; E-mail: martin.albrecht@ucd.ie*

† Electronic Supplementary Information (ESI) available: spectra of all compounds, electrochemical analyses, perspective views of the structures, and crystallographic data. See DOI: 10.1039/b000000x/

1 For representative examples, see: a) K. Kalyanasundaram, *Coord. Chem. Rev.,* 1982, **46**, 159–244; b) A. Juris, V. Balzani, F. Barigelletti, S. Campagna, P. Belser and A. von Zelewsky, *Coord. Chem. Rev.*, 1988, **84**, 85–277; c) M. D. Purugganan, C. V. Kumar, N. J. Turro and J. K. Barton, *Science,* 1988, **241**, 1645–1649; d) V. Balzani and A. Juris, *Coord. Chem. Rev.*, 2001, **211**, 97–115; e) M. M. Richter, *Chem. Rev.,* 2004, **104**, 3003–3036. f) N. C. Fletcher, *J. Chem. Soc., Perkin Trans. 1,* 2002, 183–1842; g) E. C. Constable, *Chem. Soc. Rev.*, 2007, **36**, 246–253; h) M. D. Ward, *Chem. Commun.*, 2009, 4487–4499; i) B. M. Zeglis, J. A. Boland and J. K. Barton, *Biochemistry*, 2009, **48**, 839–849; j) W. J. Youngblood, S.-H. A. Lee, K. Maeda and T. E. Mallouk, *Acc. Chem. Res.*, 2009, **42**, 1966–1973; k) J. Desilvestro, M. Grätzel, L. Kavan, J. E. Moser and J. Augustynski, *J. Am. Chem. Soc.*, 1985, **107**, 2988–2990; l) A. Hagfeldt and M. Grätzel, *Acc. Chem. Res.*, 2000, **33**, 269–277; m) M. Grätzel, *Inorg. Chem.*, 2005, **44**, 6841–6851; n) B. Schulze, D. Escudero, C. Friebe, R. Siebert, H. Görls, S. Sinn, M. Thomas, S. Mai, J. Popp, B. Dietzek, L. González and U. S. Schubert, *Chem. Eur. J.*, 2012, **18**, 4010–4025; o) D. Brown, N. Sanguantrakun, B. Schulze, U. S. Schubert and C. Berlinguette, *J. Am. Chem. Soc.*, 2012, **134**, 12354–12357.

2 a) A. Hagfeldt, G. Boschloo, L. Sun, L. Kloo and H. Pettersson, *Chem. Rev.*, 2010, **110**, 6595–6663; b) A. P. de Silva, D. B. Fox, T. S. Moody and S. M. Weir, *Pure Appl. Chem.,* 2001, **73**, 503–511; c) N. Robertson and C. A. McGowan, *Chem. Soc. Rev.,* 2003, **32**, 96–103; d) A. O. Adeloye and P.A. Ajibade, *Int. J. Mol. Sci.*, 2010**, 11**, 3158–3176.

3 a) J.-P. Sauvage, J.-P. Collin, J.-C. Chambron, S. Guillerez and C. Coudret, *Chem. Rev.,* 1994, **94**, 993–1019; b) G. R. Newkome, T. J. Cho, C. N. Moorefield, P. P. Mohapatra and L. A. Godinez, *Chem. Eur. J.*, 2004, **10**, 1493–1500; c) L. Mercs, A, Neels, H. Stoeckli-Evans and M. Albrecht, *Inorg. Chem.*, 2011, **50**, 8188–8196; d) M. Nussbaum, O. Schuster and M. Albrecht, *Chem. Eur. J.*, 2013, **19**, in press.

4 a) C. W. Jiang, H. Chao, X. L. Hong, H. Li, W. J. Mei and L. N. Ji, *Inorg. Chem. Commun.*, 2003, **6**, 773–775; b) D. Ossipov, S. Gohil and J. Chattopadhyaya, *J. Am. Chem. Soc.,* 2002, **124**, 13416–13433; c) H. Chao, W. H. Mei, Q. W. Huang and L. N. Ji, *J. Inorg. Biochem.*, 2002, **92**, 165–170.

5 a) P. G. Jessop, F. Joo and C. C. Tai, *Coord. Chem. Rev.,* 2004, **248**, 2425–2442; b) F. R. Keene, *Coord. Chem. Rev.,* 1999, **187**, 121–149; c) S. I. Murahashi and N. Komiya, *Ruthenium in Organic Synthesis*, Wiley-VCH, Weinheim, Germany, 2004; d) X. Sala, I. Romero, M. Rodriguez, L. Escriche and A. Llobet, *Angew. Chem., Int. Ed.,* 2009, **48**, 2842–2852; e) L. Duan, L. Tong, Y. Xu and L. Sun, *Energy Environ. Sci.,* 2011, **4**, 3296–3313; f) L. Duan, F. Bozoglian, S. Mandal, B. Stewart, T. Privalov and A. Llobet, L. Sun, *Nat. Chem.,* 2012, **4**, 418–423.

6 C. Sens, I. Romero, M. Rodríguez, A. Llobet, T. Parella and J. Benet-Buchholz, *J. Am. Chem. Soc.*, 2004, **126**, 7798–7799.

7 J. García-Antón, R. Bofill, L. Escriche, A. Llobet and X. Sala, *Eur. J. Inorg. Chem.*, 2012, 4775–4789.

8 a) M. Suzuki, H. Furutachi and H. Okawa, *Coord. Chem. Rev.,* 2000, **200**–**202**, 105–129; b) A. L.Gavrilova and B. Bosnich, *Chem. Rev.,* 2004, **104**, 349–383; c) A. L. Gavrilova, C. J. Qin, R. D. Sommer, A. L. Rheingold and B. Bosnich, *J. Am. Chem. Soc.,* 2002, **124**, 1714–1722; d) C. Incarvito, A. L. Rheingold, A. L. Gavrilova, C. J. Qin and B. Bosnich, *Inorg. Chem.,* 2001, **40**, 4101–4108; e) J. A. Kitchen and S. Brooker, *Coord. Chem. Rev.*, 2008, **252**, 2072–2092; f) C. Di Giovanni, L. Vaquer, X. Sala, J. Benet.Buchholz, A. Llobet, *Inorg. Chem*., 2013, **52**, 4335–4345; g) J. Olguin, M. Kalisz, R. Clérac and S. Brooker, *Inorg. Chem.,* 2012, **51**, 5058–5069.

9 a) N. S. Hush *Prog. Inorg. Chem.,* 1967, **8**, 391–444; b) H. Taube, *Angew. Chem. Int. Ed. Engl.,* 1984, **23**, 329–330; c) N. S. Hush, *Coord. Chem. Rev.,* 1985, **64**, 135–157; d) C. Creutz, M. D. Newton and N. Sutin, *J. Photochem. Photobiol. A,* 1994, **82**, 47; e) B. S. Brunschwig, C. Creutz, and N. Sutin, *Chem. Soc. Rev.,* 2002, **31**, 168–184.

10 W. R. Browne, R. Hage, J. G. Vos, *Coord. Chem. Rev.*, 2006, **250**, 1653−1668.

11 N. Planas, G. J. Christian, E. Mas-Marza, X. Sala, X. Fontrodona, F. Maseras and A. Llobet, *Chem. Eur. J*., 2010, **16**, 7965–7968.

12 C. Gottardo, T. M. Kraft, M. S. Hossain, P. V. Zawada and H. M. Muchall, *Can. J. Chem.*, 2008, **86**, 410–415.

13 A. Hirsch and D. G. Orphanos, *Can. J. Chem*., 1966, **44**, 1551–1554.

14 R. Chinchilla and C. Najera, *Chem. Soc. Rev.*, 2011, **40**, 5084–5121.

15 a) K. V. Gothelf and K. A. Jorgensen, *Chem. Rev.*, 1998, **98**, 863–909; b) V. V. Rostovtsev, L. G. Green, V. V. Fokin and K. B. Sharpless, *Angew. Chem., Int. Ed.,* 2002, **41**, 2596–2599; b) F. Himo, T. Lovell, R. Hilgraf, V. V. Rostovtsev, L. Noodleman, K. B. Sharpless and V. V. Fokin, *J. Am. Chem. Soc*., 2005, **127**, 210–216.

16 For reviews, see: a) V. D. Bock, H. Hiemstra and J. H. van Maarseveen, *Eur. J. Org. Chem.*, 2006, 51–68; c) J. E. Moses and A. D. Moorhouse, *Chem. Soc. Rev*., 2007, **36**, 1249–1262; d) M. Meldal and C. W: Tornøe, *Chem. Rev*., 2008, **108**, 2952–3015; e) J. E. Hein and V. V. Fokin, *Chem. Soc. Rev*., 2010, **39**, 1302–1315. For themed issues, see: f) M. G. Finn and V. V. Fokin (Eds.), *Chem. Soc. Rev.*, 2010, **39**, 1231; g) J. Kosmrlj (Ed.), *Top. Hetercycl. Chem.,* 2012, **28**, 1; h) *Aust. J. Chem.* 2007, **60**, 381.

17 a) J. T. Fletcher, B. J. Bumgarner, N. D. Engels and D. A. Skoglund, *Organometallics*, 2008, **27** , 5430–5433; b) M. J. D. Bosdet, W.E. Piers*,* T.S. Sorensen and M. Parvez, *Can. J. Chem.*, 2010, **88**, 426–433.

18 P. Appukkuttan, W. Dehaen, V. V. Fokin and E. Van der Eycken, *Org. Lett.*, 2004, **6**, 4223–4225.

19 B. Dervaux and F. E. Du Prez, *Chem. Sci*., 2012, **3**, 959–966.

20 Phthalazine: pK_b = 10.5 ; triazole pK_b = 9.4, see: T. L. Gilchrist, *Heterocyclic Chemistry* (3rd Ed.), Prentice Hall, New Jersey, USA, 1997, pp. 432.

21 a) P. Mathew, A. Neels and M. Albrecht, *J. Am. Chem. Soc.*, 2008, **130**, 13534–13535; b) K. F. Donnelly, A. Petronilho and M. Albrecht, *Chem. Commun.*, 2013, **49**, 1145–1159.

22 D. J. Wasylenko, C. Ganesamoorthy, B. D. Koivisto and C. P. Berlinguette, *Eur. J. Inorg. Chem.,* 2010, 3135–3142.

23 Y. Xu, A. Fischer, L. Duan, L. Tong, E. Gabrielsson, B. Åkermark and L. Sun, *Angew. Chem. Int. Ed.*, 2010, **49**, 8934 –8937.

24 a) M. Albrecht, *Science*, 2009, **326**, 532–533; b) J. D. Crowley, A.-L. Lee and K. J. Kilpin, *Aust. J. Chem.*, 2011, **64**, 1118–1132; c) A. Krüger and M. Albrecht, *Chem. Eur. J.*, 2012, **18***,* 652–658.

25 R. F. Heck, *Palladium Reagents in Organic Synthesis*, Academic Press, London, 1985.

26 B. P. Sullivan, J. M. Calvert and T. M. Meyer, *Inorg. Chem.*, 1980, **19**, 1404–1407.

27 A. L. Spek, *J. Appl. Cryst.*, 2003, **36**, 7–13.

28 G. M. Sheldrick, *Acta Cryst.*, 2008, *A***64**, 112–122.

for TOC entry only:

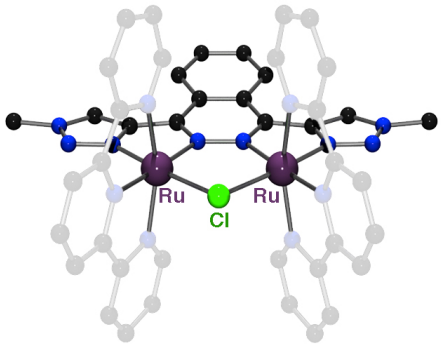

A new phthalazine-bis(triazole) ligand has been developed that provides a suitable binding pocket for coordinating two ruthenium(II) centers in a coaxial octahedral RuN5Cl environment, enabling the metals to efficiently communicate with each other.